Supporting Information

Experimental

Reagents. Colloidal silica (Ludox, 40 wt.% in H_2O) was purchased from Alfa Aesar. Tetrapropyl ammonium hydroxide (TPAOH, 25 wt.% in H_2O) and $Al(NO_3)_3 \cdot 9H_2O$ were purchased from Sinopharm Chemical Reagent Co.,LTD. All chemicals were used as received.

Methods.

Synthesis of mesoporous ZSM-5 nanocrystals: A mixture of $100SiO_2$/25-$100TPAOH$/0.125-$1Al_2O_3$/62-$150H_2O$ was transferred to a Teflon-lined autoclave and crystallized at 120 °C for 0-72 h. After crystallization, the products were dried and then heated at 550 °C in air for 6 h to remove organic components. All these calcinated samples were exchanged to H-form with NH_4NO_3 (1.0 M) at 80 °C for 5 h and three times, followed by drying and calcinating in air at 500 °C. These samples were designated as mZx-y, x is the molar ratio of Si/Al and y is the molar ratio of Si/TPAOH. Detailed reaction parameters were listed in Table S1.

Table S1. Synthesis conditions of various mesoporous ZSM-5 nanocrystals.

Samples	mZ50-1	mZ50-2	mZ50-4	mZ100-4	mZ200-4	mZ400-4
Si/Al (molar ratio)	50	50	50	100	200	400
Si/TPAOH (molar ratio)	1	2	4	4	4	4
$(SiO_2+Al(NO_3)_3+TPAOH)/H_2O$ (weight ratio)	10	10	10	10	10	10
temperature (°C)	120	120	120	120	120	120
reaction time (h)	48	48	0-72	48	48	48

Synthesis of bulk sample: The bulk sample was synthesized from a clear precursor sol composed of $100TEOS/20TPAOH/2NaAlO_2/5500H_2O$ and then crystallized at 170 °C for 72 h. The as-synthesized sample was washed with distilled water and heated at 550

°C in air for 6 h to remove organic components. The calcinated sample was exchanged to H-form with NH_4NO_3 (1.0 M) at 80 °C for 5 h and three times, followed by drying and calcinating in air at 500 °C. The obtained sample was designated as bulk50, 50 is the molar ratio of Si/Al.

Characterizations. The powder X-ray diffraction (XRD) patterns were recorded on a Rigaku D/ Max 2550 X-ray diffractometer with Cu Kα radiation (λ= 1.5406 Å) with a tube current of 30 mA and a tube voltage of 40 kV. The scanning electron microscope (SEM) images were taken on a JEOL JSM-6700 F field emission scanning electron microscope and the spatial distribution of the elemental composition in the zeolite crystals were measured using SEM-EDX in a JEOL JSM 6700 F microscope. The transmission electron microscopy (TEM) images were obtained on a JEM-200CX transmission electron microscope. The nitrogen adsorption/desorption measurements were performed on a NOVA 2200e Accelerated Surface Area and Porosimetry (Quantachrome Inc., USA). The ^{27}Al solid-state nuclear magnetic resonance (NMR) experiments were performed on Bruker AVANCE III 400WB spectrometer. The spectra were collected with a frequency of 104.3 MHz for ^{27}Al. The diffuse reflectance infrared Fourier transform (DRIFT) spectroscopic analyses were carried out with Nicolet 6700 Fourier spectrophotometer in the transmission mode at 723 K using flowing Ar and were presented in absorbance. The content of Al in ZSM-5 was determined by Inductively Coupled Plasma (ICP, Thermo iCAP6300) and Shimadzu Sequential X-ray Fluorescence Spectrometer (XRF-1800). Acidic properties of zeolites were measured by temperature-programmed desorption of ammonia (NH_3 -TPD) method. 0.1 g samples were purged with pure He at 300 °C for 1 h, and then cooled to room temperature. After being saturated with NH_3 , the samples were flushed by pure He at 100°C for 30 min. Then, the samples were heated to 650 °C at ramp rate of 10 °C and the signals were monitored by a thermal conductivity detector (TCD).

Catalytic reactions. The catalytic reaction of methanol to propylene (MTP) was performed in a fixed-bed reactor under atmospheric pressure. Typically, 0.2 g of the sample was loaded into a tube quartz reactor and purged with N_2 at 460 °C for 1 h. After that, the reaction was carried out at 460 °C and the weight hourly space velocity

(WHSV) for methanol was 1.25/2.5 g g^{-1} h^{-1} with a feed of methanol solution ($n(CH_3OH):n(H_2O)$ = 1:5). The total products were analyzed by an on-line gas chromatograph (Shimadzu, GC-2014) equipped with a Flame Ionization Detector (FID) and a Rt-Q-BOND PLOT capillary column in length of 30 m. Both methanol and dimethylether (DME) were regarded as reactants for calculation.

Figures

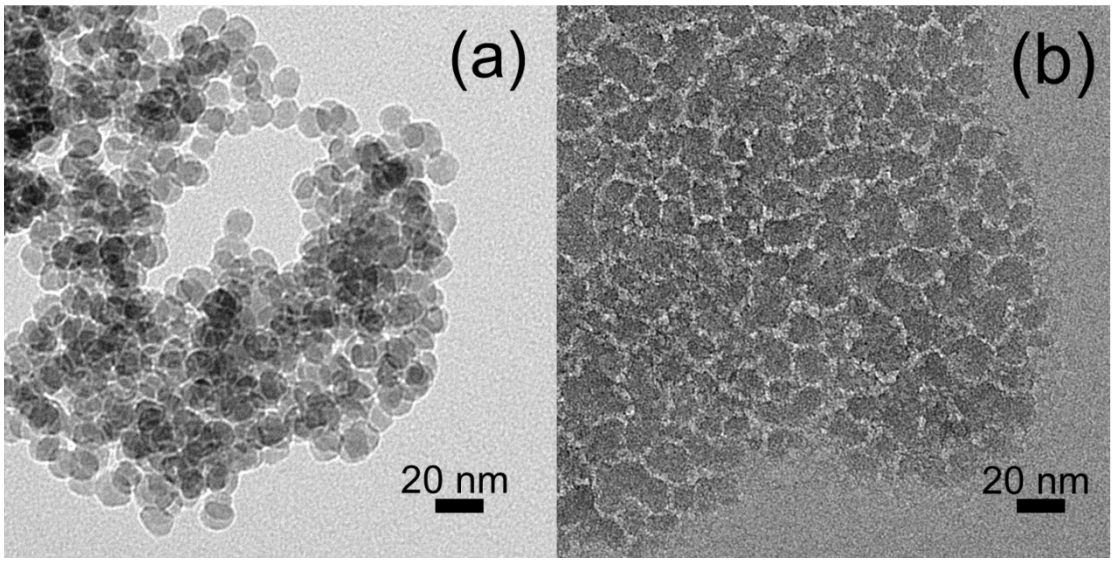

Figure S1. TEM images of (a) Ludox and (b) homogeneous colloid of aluminosilicate gel. It was obviously that the mean size of silica nanoparticles in commercial Ludox was 14 nm. After mixing with aluminum source and TPAOH, a homogeneous aluminosilicate was obtained.

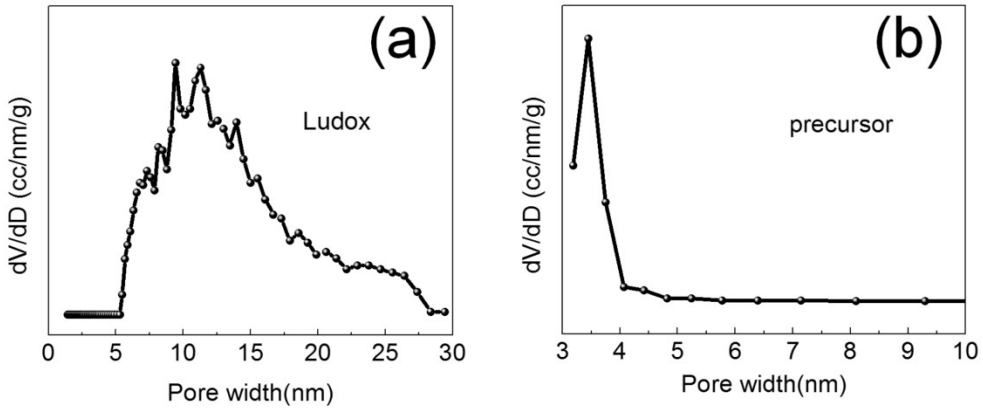

Figure S2. Pore size distribution of Ludox (a) and precursor (b). The size of voids among precursor was centered at 3-6 nm, which is smaller than that of the Ludox aggregates (5-28 nm). This observation suggests the TPA^+ species have penetrate the amorphous aluminosilicate gel resulting in partially etching of silica for further growth of zeolite. Kirkendall growth was used here to reserve these inter-particle voids.

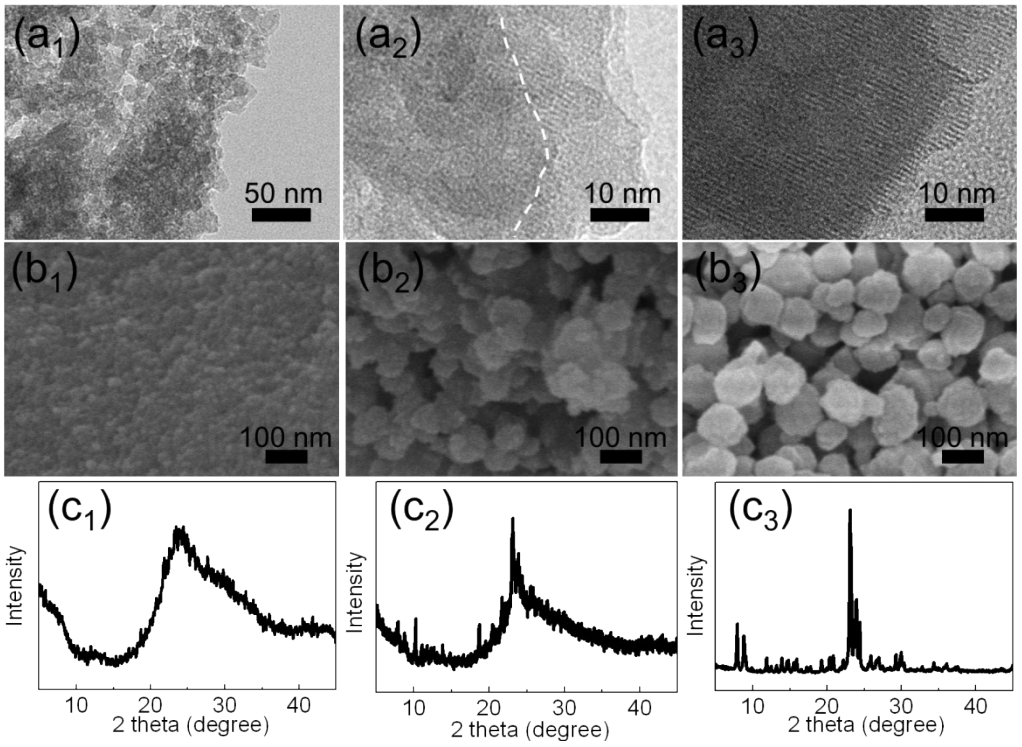

Figure S3. Kirkendall growth of mZ50-4. TEM images (a), SEM images (b) and XRD patterns (c) of typical samples taken at different time intervals of 0 h (a_1-c_1), 4 h (a_2-c_2) and 12 h (a_3-c_3). Crystallization process was proceeded with the presence of limited amounts of water. With the crystallization proceeded, the water vapor diffused gradually from outside in, resulting in the merge of initial gel (b_1) into secondary particles (b_2). Simultaneously, the diffusion of water vapor triggered crystallization of amorphous aluminosilicate gel intermediates with the help of TPAOH and thus formed ZSM-5. The obvious interface (a_2) between as-formed zeolite and amorphous intermediates thus formed, unambiguously demonstrating the nanoscale Kirkendall growth here. Nanovoids simultaneously diffused into ZSM-5, generating mesopores in situ. Meanwhile, the adjacent aluminosilicate gel were merged together at the earlier stage of crystallization process (b_2), resulting in the formation of secondary nanoparticles (b_3).The process was also reflected by XRD pattern with changing from amouphouse phase (c_1) to weak characteristic peaks (c_2) assigned to MFI structure. Further crystallization procedure generates ZSM-5 particles with mesopores as shown in a_3, b_3 and c_3.

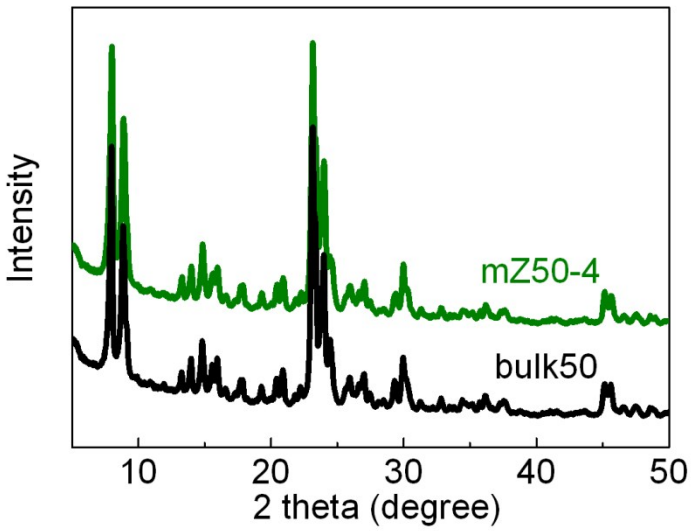

Figure S4. XRD patterns of mZ50-4 and bulk50.

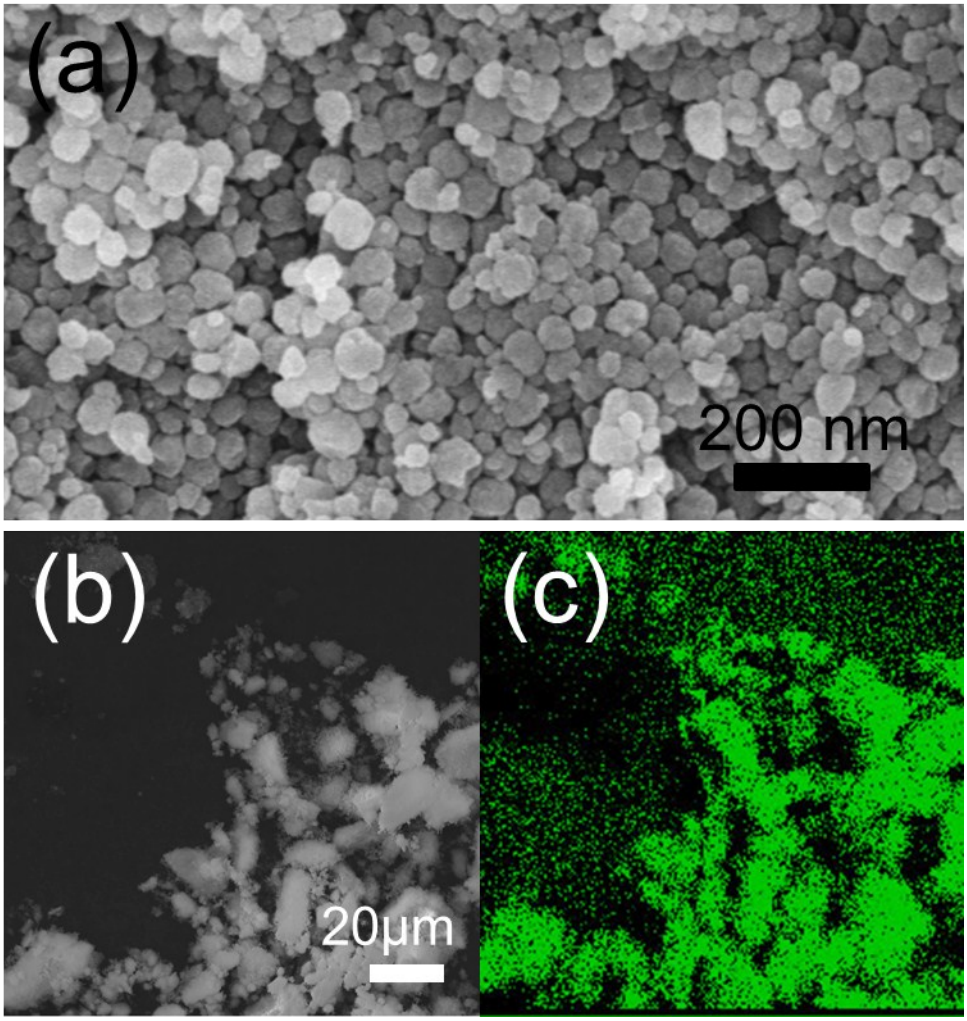

Figure S5. SEM image (a and b) and the corresponding elemental mapping image of mZ50-4.

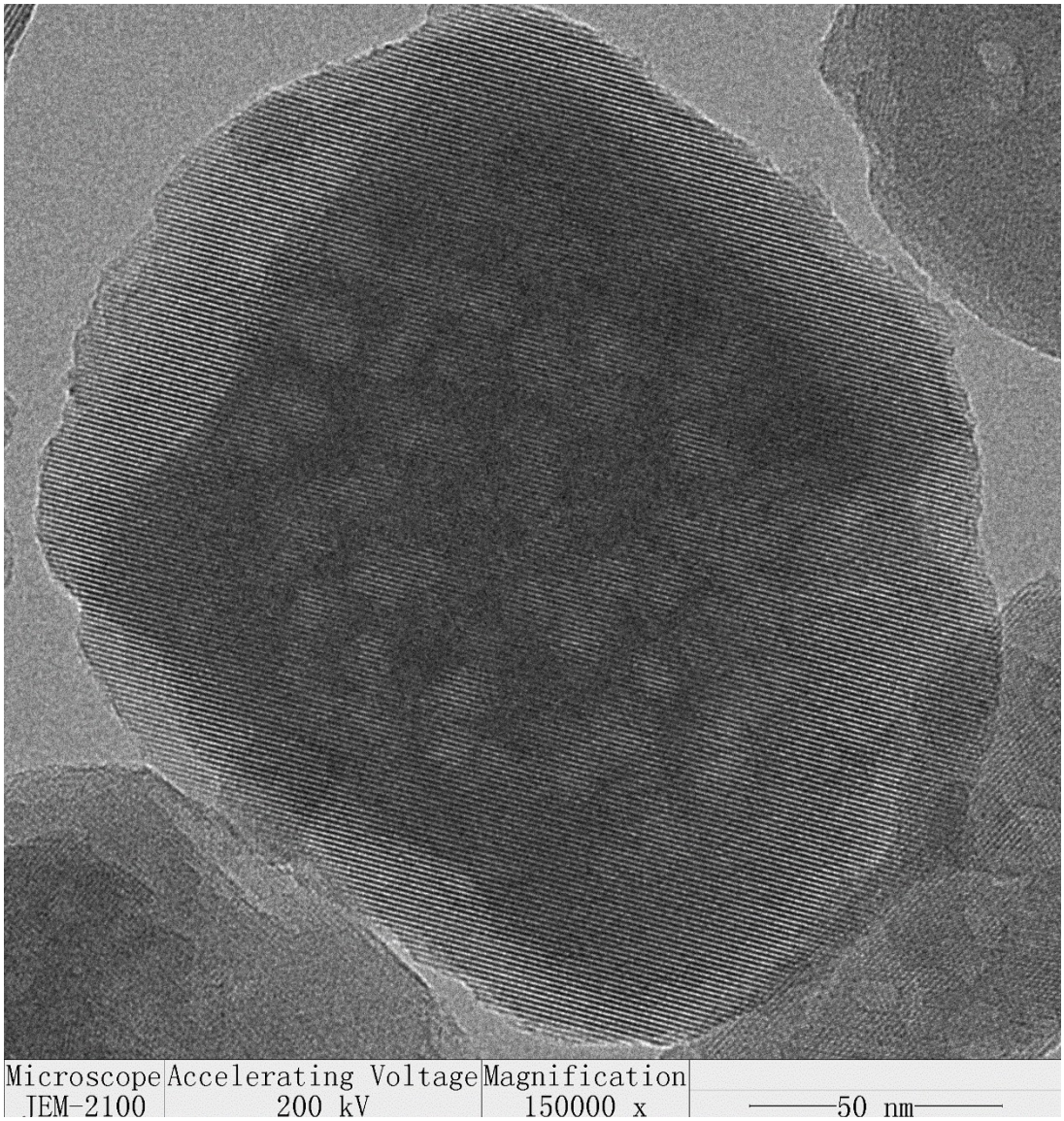

Figure S6. High resolution TEM (HRTEM) image of mZ50-4.

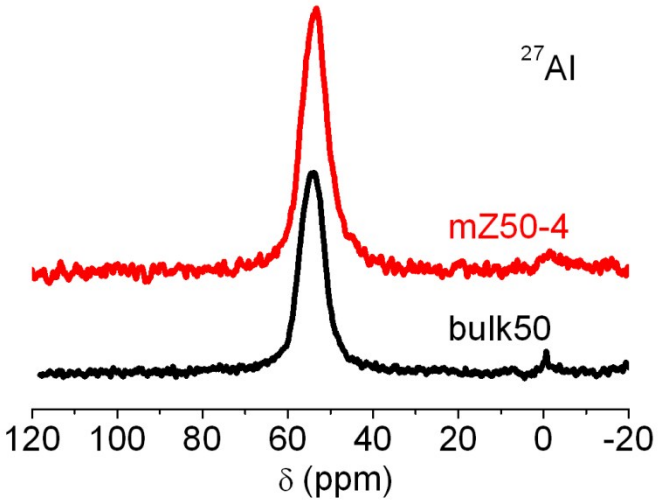

Figure S7. ^{27}Al NMR MAS spectra of the mZ50-4 and control sample. Both the samples exhibit band at δ = 55 ppm corresponded to aluminum species with tetrahedral coordination. Furthermore, signals at δ = 0 ppm was negligible, indicating that the Al atoms are mostly incorporated into the crystalline frameworks.

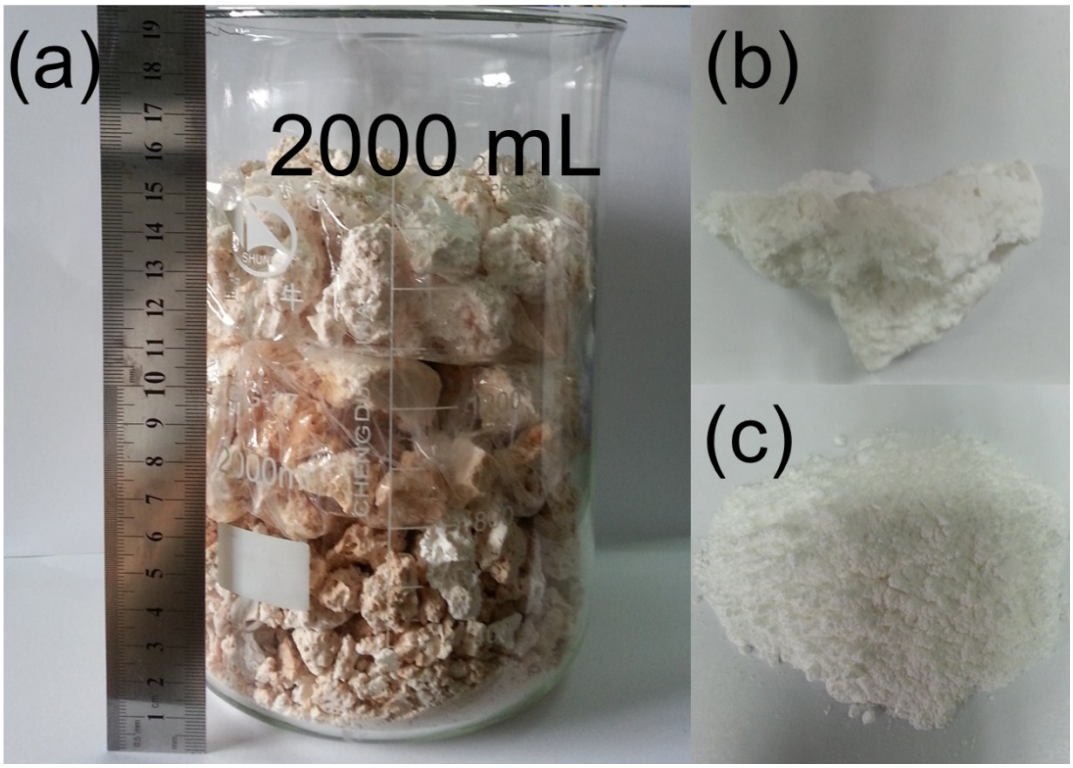

Figure S8. (a) Photo of mZ50-4 sample (1000 g, without calcination) synthesized by Kirkendall method. The white color of the monoliths product (b) and corresponding powder (c) suggest organic components can be removed clearly even without washing process.

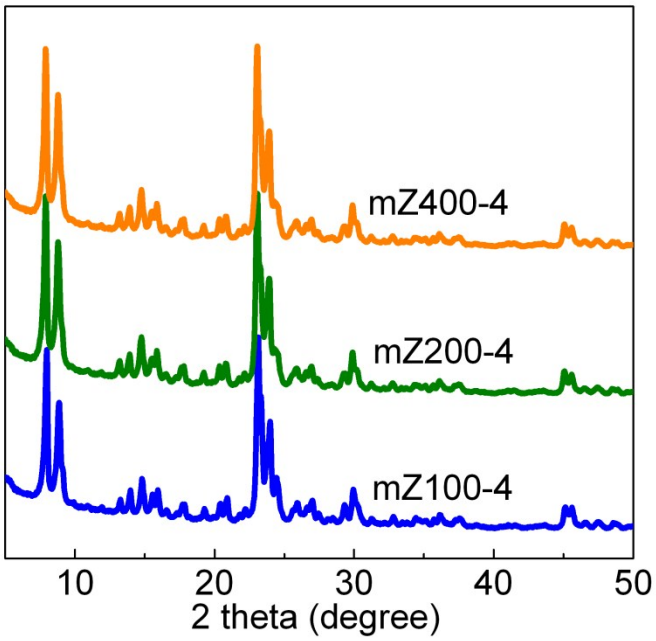

Figure S9. XRD patterns of mesoporous ZSM-5 with various Si/Al ratios.

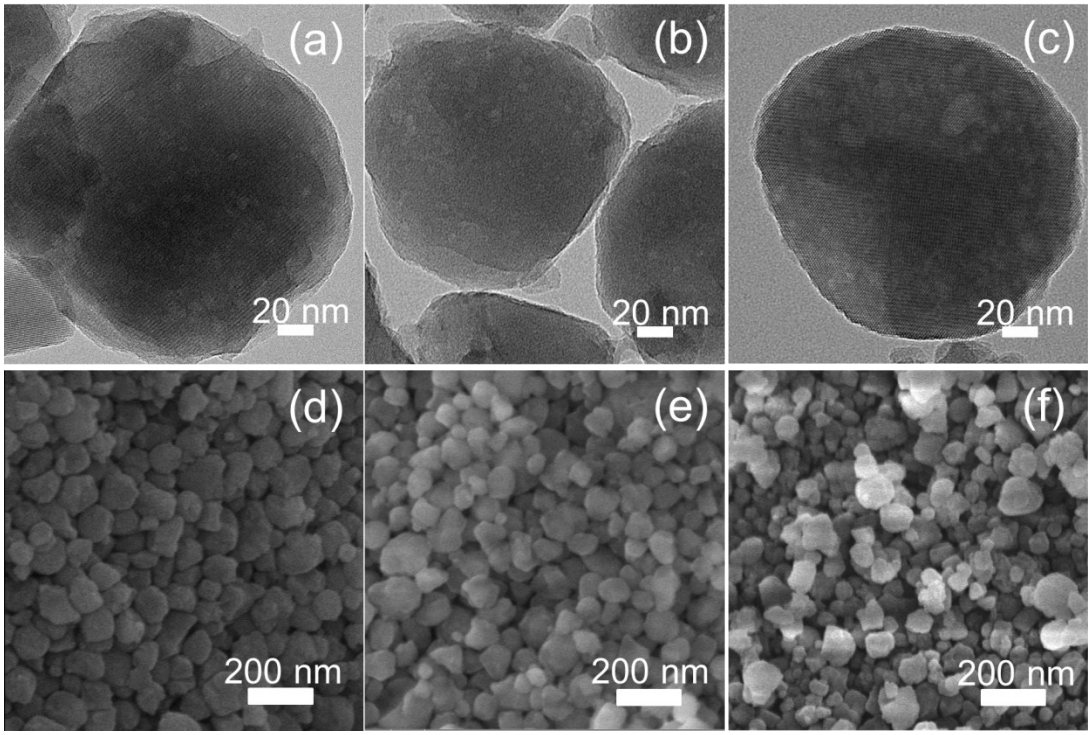

Figure S10. The TEM images and SEM images of samples with various Si/Al ratios: mZ100-4 (a, d), mZ200-4 (b, e) and mZ400-4 (c, f).

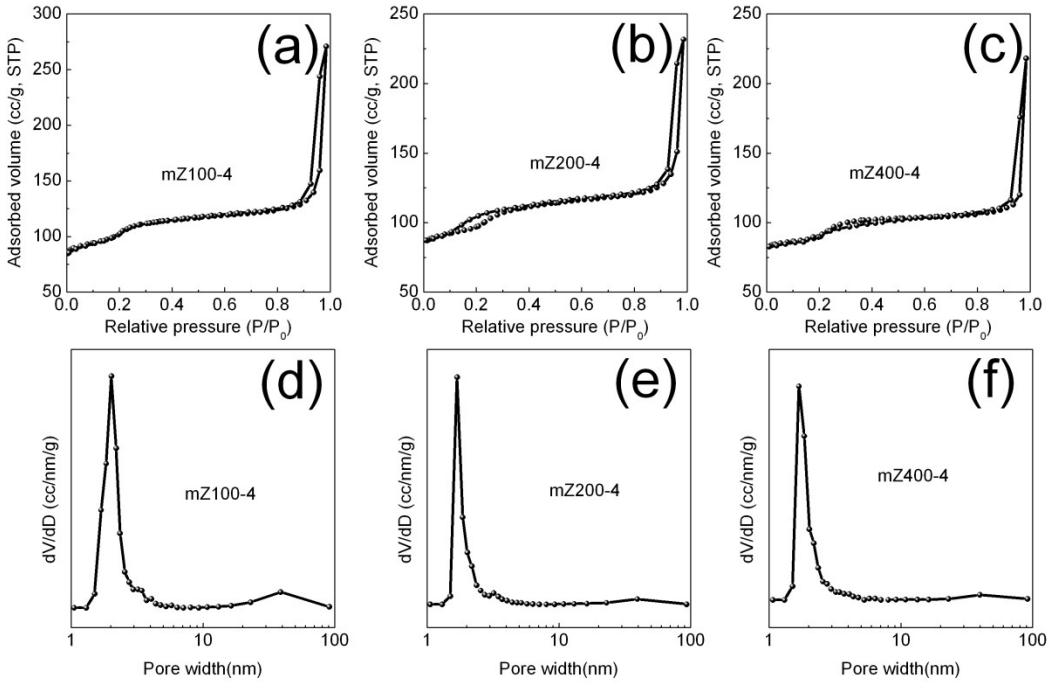

Figure S11. The N_2 adsorption-desorption isotherm and the corresponding BJH pore size distribution of mZ100-4 (a, d), mZ200-4 (b, e) and mZ400-4 (c, f).

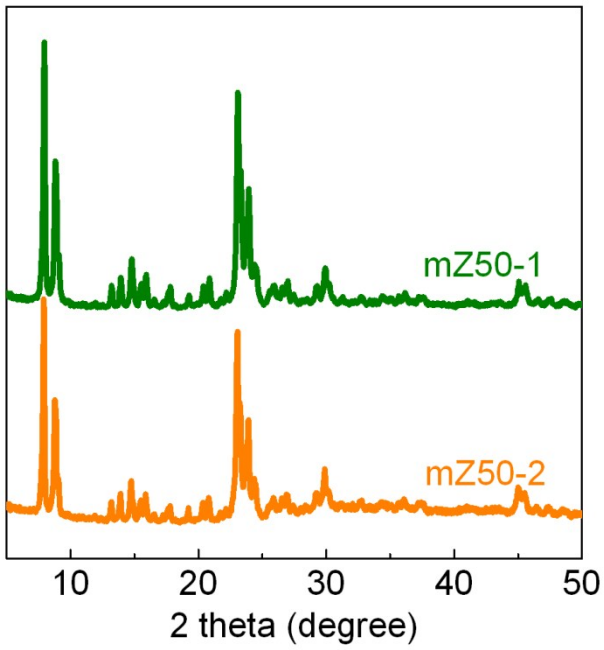

Figure S12. XRD patterns of mZ50-2 and mZ50-1.

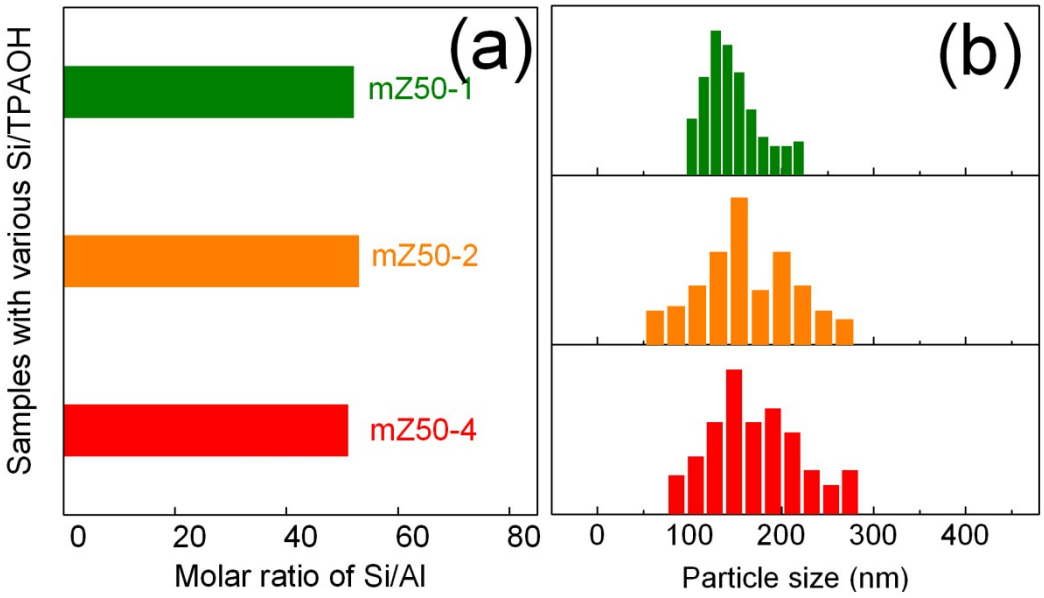

Figure S13. The Si/Al ratio (a) and particle size distributions (b) of samples with various Si/TPAOH ratios.

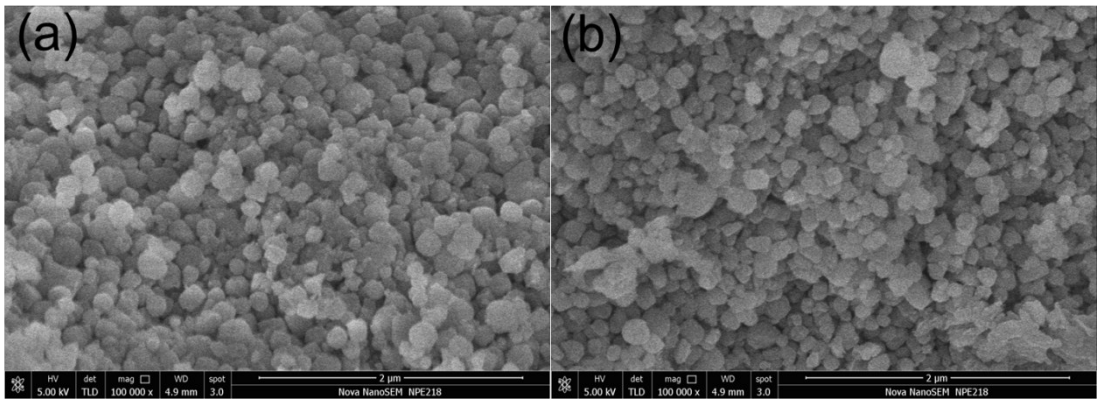

Figure S14. SEM images of (a) mZ50-2 and (b) mZ50-1.

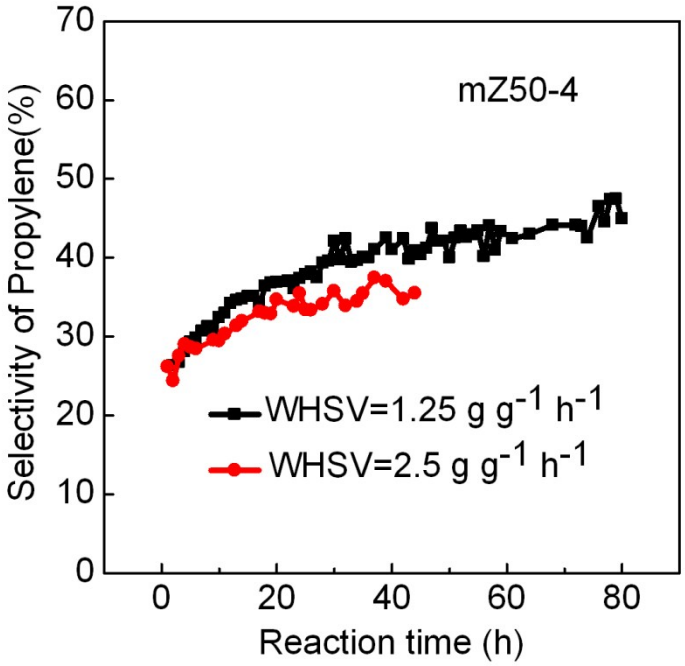

Figure S15. Propylene selectivity of mZ50-4 under different WHSV of 1.25 g g^{-1} h^{-1} and 2.5 g g^{-1} h^{-1} with other conditions fixed: T = 460 °C, n(CH_3OH) : n(H_2O) = 1 : 5, P_{total} = 1 atm. It suggested that the propylene selectivity remained while the WHSV changed.

Table S2. Synthesis conditions and the pore volumes of various ZSM-5.

Sample	SDA[a]	Template	V_{total}[b] (cc/g)	V_{micro}[c] (cc/g)	Ref.
meso-50	TPAOH[d]	/	0.48	0.13	Our work*
meso-100	TPAOH	/	0.42	0.13	Our work
meso-200	TPAOH	/	0.36	0.14	Our work
meso-400	TPAOH	/	0.34	0.13	Our work
ZSM-5 hollow fibers	TPAOH	PVP[e]	0.41	0.10	10
3DOm-i MFI	TPAOH	3DOm carbon[f]	0.33	0.14	S1
Meso-ZSM-5	TPAOH	NDCs[g]	0.30	0.13	S2
P-C_{22}-MFI	$C_{22\text{-}6\text{-}0}Br$[h]	/	0.44	0.136	S3
SCZN-2	$BC_{Ph\text{-}6\text{-}6\text{-}6}$[i]	/	0.51	0.11	S4

*Samples obtained with molar ratio of SiO_2/TPAOH to be 4/1, weight ratio of dry gel/water to be 10/1, at 120 °C for 48 h.

a: Structure directing agent

b: Total pore volume

c: Micropore volume

d: Tetrapropylammonium hydroxide, a conventional structure directing agent

e: Polyvinylpyrrolidone (PVP, Mw ≈1,300,000)

f: Three-dimensionally ordered mesoporous carbon

g: N-doped carbonaceous monoliths

h: $[C_{22}H_{45} - N^+(CH_3)_2 - C_6H_{12} - N^+(CH_3)_2 - C_6H_{13}]Br_2$, an organic surfactant functionalized with a diquaternary ammonium group in the head

i: $C_6H_{13} - N^+(CH_3)_2 - C_6H_{12} - N^+(CH_3)_2 - (CH_2)_6 - O - C_6H_4 - C_6H_4 - O - (CH_2)_6 - N^+(CH_3)_2 - C_6H_{12} - N^+(CH_3)_2 - C_6H_{13}$ ($4Br^-$), a bolaform amphiphilic molecule with bi-quaternary ammonium head groups and biphenyl groups

Table S3. NH_3-TPD and ICP/XRF data of different ZSM-5 zeolites

Samples	Total (mmol/g)	Weak (mmol/g)	Strong (mmol/g)	Si/Al (molar ratio)
mZ50-4	0.980	0.430	0.550	51
bulk50	0.904	0.546	0.358	53

Table S4. ICP/XRF data of ZSM-5 with various Si/Al ratios.

Samples	mZ50-4	mZ100-4	mZ200-4	mZ400-4
Si/Al (molar ratio)	51	95	173	370

S1. Chen, H.; Wydra, J.; Zhang, X.; Lee, P. S.; Wang, Z.; Fan, W.; Tsapatsis, M. *J. Am. Chem. Soc.* **2011**, 133, 12390-12393.

S2. White, R. J.; Fischer, A.; Goebel, C.; Thomas, A. *J. Am. Chem. Soc.* **2014**. 136, 2715-2718.

S3. Na, K.; Choi, M.; Park, W.; Sakamoto, Y.; Terasaki, O.; Ryoo, R. *J. Am. Chem. Soc.* **2010**, 132, 4169-4177.

S4. Xu, D.; Ma, Y.; Jing, Z.; Han, L.; Singh, B.; Feng, J.; Shen, X.; Cao, F.; Oleynikov, P.; Sun, H. *Nat. Commun.* **2014**, 5, 1-9.